Hindawi
Journal of Advanced Transportation
Volume 2021, Article ID 4310403, 13 pages
https://doi.org/10.1155/2021/4310403

Research Article

A Multiroute Signal Control Model considering Coordination Rate of Green Bandwidth

Jiao Yao,[1] **Qingyun Tang**,[1] **and Pincheng Wang**[2]

[1]*Business School, University of Shanghai for Science and Technology, Shanghai 200093, China*
[2]*CCDI (Suzhou) Exploration & Design Consultant Co., Ltd., Suzhou, Jiangsu 215123, China*

Correspondence should be addressed to Jiao Yao; yaojiao@126.com

Received 27 September 2021; Revised 16 November 2021; Accepted 23 November 2021; Published 14 December 2021

Academic Editor: Socrates Basbas

Oriented to characteristics of the inflow and outflow of routes in urban road network, we modified the classical fundamental green wave bandwidth model, in which separate turning green wave band is available for traffic flow from subarterials merging into an arterial, and this variable green wave band can be more flexible to service the commuting traffic. Moreover, with the analysis of the mapping characteristics of the phase coordination rate, the concept of the coordination rate of green wave bandwidth was proposed, with which as the objective function, a multiroute signal coordination control model was established, and this model is a mixed integer linear programming problem with the overall optimal coordination rate of inbound, outbound, and turning movement as the objective. Finally, a case study was given with road network in Suzhou Industrial Park, Jiangsu Province, China. From the simulation results, we can conclude that the coordinated distribution of the model proposed in this study is more stable; the fluctuation range is 0.09, which is less than that of optimization scheme in classical signal timing software Synchro, which is 0.33; and the total route delay can also be reduced by 15% compared to the current situation and 3.3% compared to Synchro optimization solution.

1. Introduction

Nowadays, traditional coordinated control in arterials gradually cannot meet the increasing demand for commuting, where there are often multiple routes to choose from the origin (such as home) to the destination (such as work place). Therefore, in addition to the study of the coordinated control in arterials, the inflow and outflow of the traffic in commuting OD, such as turning movements, are considered in the multiroute in road network.

Green wave control is one of the classical and effective methods for the coordinated control in arterials and routes. The objective function is usually to find the maximum green wave bandwidth in an arterial. This model was first proposed by Litter and Gartner in 1981, namely, the MAXBAND model [1–3]. Subsequently, in order to solve the defect that the bandwidth of MAXBAND cannot be changed, Gartner et al. proposed the MULTIBAND model in 1990. This model can implement different bandwidths for different road sections and directions, and it takes into account the urban arterial traffic. When different road sections and different traffic volumes have different requirements for bandwidth, the traffic flow imbalance coefficient is added to the model [4]. Moreover, in response to the requirement of coordinated control of regional network signals, an improved MULTIBAND-96 algorithm [5] was proposed, which can optimize the solution time of the MULTIBAND model in extent larger area. However, MULTIBAND still does not change the fact that the center of the bandwidth is symmetrical. In the coordinated control of the route, the turning bandwidth is different from the straightforward bandwidth and is more complicated. Therefore, Chao et al. proposed the AM-BAND green wave model in which, by changing the symmetry coefficient of the green wave bandwidth, an asymmetric multiband model was established to maximize the utilization of the green time of each phase in arterials. In AM-BAND, each green wave band of each direction has a centerline, so the bandwidth on both directions does not have to be symmetrical along the centerline [6]. Since then, the model has been continuously developed and improved by researchers at home and aboard. Lu and Cheng improved the classic two-way green wave bandwidth graphic method by improving the arterial intersection and considering the asymmetry of the phase sequence [7]. In 2018, the OD-NETBAND model for small road networks was proposed; it created a separate green wave bandwidth for each main OD flow direction to achieve coordinated control in regional road network [8].

However, when the research object comes to multiple routes, the links between adjacent intersections are closer, and the coordination method of the maximum bandwidth method often ignores the correlation between individual intersections, resulting in discontinuity of green wave guidance. In order to reflect the mapping characteristics of adjacent intersections, the concept of green wave bandwidth coordination rate was proposed, with which as the objective function, multiroute green wave control research was also proposed, in which the phase coordination has been widely used. Katwijk et al. proposed a phase-adjustable multiagent coordinated control model, which can dynamically adjust the phase in real time according to the traffic flow of a certain phase at the current intersection [9]. Based on the mapping characteristics of adjacent intersections, An proposed the concept of phase coordination rate, which reflects the optimization of intersection through the coordination volume [10]. In addition, in view of the uneven distribution of traffic flow at intersections along arterials, Liang et al. took the overlapping phase into account and applied bus signal priority control, which has more practical significance than the traditional phase. Under certain applicable conditions, this method can reduce the total amount of passenger delay effectively at intersections along arterials [11]. Based on the design of phase coordination, Zhang et al. proposed a green wave coordinated control method in arterials based on overlapped phases to better match the arrival time of the two-way traffic flow when the green light turns on at intersections [12–17]. Lan and Wu used the method of correlation analysis and regression analysis to establish correlation model of adjacent intersections, the principle and process of traffic partition were designed by using analytic hierarchy process, and a new traffic partition model was proposed [18]. The route observed in this study was extracted from the Floating Vehicle Data (FCD) of commercial vehicles in the study area of Calabria (southern Italy). The comparison is performed based on the similarity of the sequence of nodes visited between the observation route and the simulated/optimized route [19]. Hu et al. proposed an improved HCM 2000 delay model based on the coordination of dynamic random traffic flow phase difference, using genetic particle swarm hybrid optimization algorithm to optimize the coordinated control timing scheme and realize all intersection signals in the subarea [20].

Based on the characteristics of phase coordination, this paper proposes the concept of coordination rate of green wave bandwidth. After analysis of bandwidth coordination rate of the green wave in two-way movement, straight and turning, the multiroute based control optimization model is established. In this model, constraints of the variable bandwidth, setting of the turning bandwidth, and green wave bandwidth coordination rate are taken into account comprehensively, and inbound, outbound, and turning traffic flow are also serviced at the same time in this model.

The contributions of this paper are as follows:

The basic green wave bandwidth model of the trunk line is improved to create a separate turning green wave band for the traffic flow from the branch line to the trunk line, so that the variable green wave bandwidth can be more flexibly adapted to the needs of related commuting traffic.

(1) The concept of green wave bandwidth coordination rate is introduced.
(2) This model is a mixed integer linear programming model that is aimed at the overall optimal coordination rate of green wave bandwidth for uplink, downlink, and steering.

2. Definition

Some basic concepts are defined first as follows:

Route: the path is a line composed of several intersections and road sections from the start to the end of commuter traffic.

Multipath: since there are multiple start and end points in the road network, multiple paths appear.

Green bandwidth: route may have multiple intersections, along which we can adjust the offset of green time of traffic lights to make the traffic passing through several intersections without stop, which we call green wave. The duration of the green wave is the green wave bandwidth.

2.1. Intersection Phase Coordination Rate.

When describing the characteristics of adjacent intersections, the concept of phase difference is usually used. Phase difference is also an important indicator for coordinated control of trunk lines. The phase coordination rate reflects the mapping relationship of the green light phase duration of adjacent intersections.

2.1.1. The Concept of Phase Coordination Rate.

The phase coordination rate is defined as the degree of coincidence of the green light time interval of a certain phase at the upstream intersection to the downstream intersection and the coincidence degree of the green light time interval of the corresponding phase at the downstream intersection.

Take the straight phase of the adjacent intersection as an example, as shown in Figure 1.

The figure shows two adjacent intersections $I_{i,j}$ and $I_{i+1,j}$; $G_{i+1,j}$ and $G_{i,j}$ are the straight phase green time (s) of the upstream and downstream intersections in the same cycle; $O_{i+1,j}$ is the difference between the green light start times of adjacent intersections (phase difference); $\xi_{i+1,j}$ is the phase noncoordination amount (s), that is, the part that does not coincide with the downstream green light time after the upstream intersection is mapped; $\varphi_{i+1,j}$ is the phase coordination amount (s), that is, the overlapped part of the upstream intersection and the downstream green light time after the mapping.

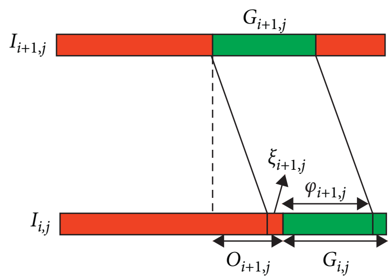

Figure 1: Schematic diagram of phase coordination rate.

Therefore, the calculation method of the straight-going phase coordination rate γ at the two intersections in the figure is shown in

$$\gamma_{i+1,j} = \frac{\varphi_{i+1,j}}{\varphi_{i+1,j} + \xi_{i+1,j}}. \quad (1)$$

2.1.2. Intersection Control Optimization Model Based on Phase Coordination Rate. The phase coordination rate is calculated strictly according to the number of phases, taking the standard four-phase signal control (go straight from east to west, turn left from east to west, go straight from north to south, and turn left from north to south) as an example (for the time being, complex situations such as phase overlap are not considered), and the phase coordination rate needs to be calculated for each phase.

When calculating the coordination rate for a phase, since the traffic flow is bidirectional, the coordination rate of the phase is defined as the larger of the two, as shown in the following formula (assuming the phase is an east-west straight phase).

$$\gamma_{i+1,j} = \max\left(\gamma_{i+1,j}^{e\longrightarrow w} \gamma_{i+1,j}^{w\longrightarrow e}\right). \quad (2)$$

In the actual intersection, the traffic turning problem at the entrance lane of the intersection is involved. Therefore, considering the signal control environment at the intersection, the phase coordination rate optimization model is divided into two categories, namely, the phase mapping of straight to straight, and the phase of straight to left turn. The mapping is for the vehicle flow at the upstream and downstream intersections, as shown in Figure 2. The situation of mixed lanes and controlled right turn is not considered here.

2.1.3. Go Straight-Go Straight to Map the Phase Coordination Rate. As shown in the direction of the straight traffic flow in Figure 2, the traffic flow goes straight through the upstream intersection I and goes straight out of the downstream intersection II. The phase coordination rate is defined as

$$\gamma_{12}^{T} = \frac{\varphi_2^{T}}{\varphi_2^{T} + \xi_2^{T}}. \quad (3)$$

Among them, γ_{12}^{T} is the straight-going phase coordination rate, φ_2^{T} is the straight-going phase coordination

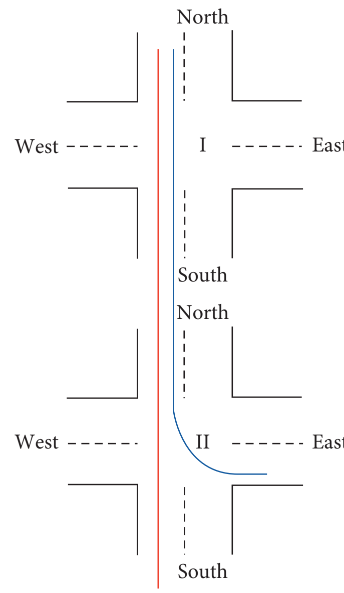

Figure 2: Traffic flow mapping trend diagram of adjacent intersections.

quantity (s), and ξ_2^{T} is the straight-going phase noncoordination quantity (s).

According to the phase mapping relationship,

$$\varphi_2^{T} + \xi_2^{T} = G_1^{T}, \quad (4)$$

where G_1^{T} is the green time of the straight phase of intersection I (s).

According to the phase difference and the phase coordination rate, the straight-line phase noncoordination rate can be obtained as shown in

$$\delta_{12}^{T} = \frac{\xi_2^{T}}{\Delta_{12}}. \quad (5)$$

Among them, Δ_{12}^{T} is the phase difference (s) between intersections I and II. When the phase noncoordination rate is 0, the effect of coordinated control is the best, which can reduce the queuing problem of vehicles.

2.1.4. Go Straight-Turn Left to Map the Phase Coordination Rate. As shown in the direction of the turning traffic flow in Figure 2, the traffic flow goes straight through the upstream intersection I and turns left out of the downstream intersection II. The phase coordination rate is defined as

$$\gamma_{12}^{L} = \frac{\varphi_2^{L}}{\varphi_2^{T} + \xi_2^{T}}. \quad (6)$$

Among them, φ_2^{L} is the left-turn phase coordination quantity (s); in phase mapping, the phase noncoordination quantity is usually constant.

2.1.5. Intersection Control Optimization Model. In the actual calculation of the phase coordination rate of a downstream intersection, the upstream intersection usually has four values for north, south, east, and west, and the corresponding traffic flow mapping conditions also come from the four directions. According to vehicle driving behavior, the coordination rate can be classified into four categories, namely, east-west straight phase coordination rate, east-west left-turn phase coordination rate, north-south straight phase coordination rate, and north-south left-turn phase coordination rate, which are represented by the following symbols: $\gamma^1_{i\longrightarrow j}$, $\gamma^2_{i\longrightarrow j}$, $\gamma^3_{i\longrightarrow j}$, and $\gamma^4_{i\longrightarrow j}$.

Then, the intersection control optimization model based on the phase coordination rate, which is aimed at the optimal total phase coordination rate of the entire downstream intersection, can be expressed as

$$\operatorname{Max} f\left(I_{i\longrightarrow j}\right) = \alpha_1\gamma^{NT}_{i\longrightarrow j} + \beta_1\gamma^{NL}_{i\longrightarrow j} + \alpha_2\gamma^{WT}_{i\longrightarrow j} + \beta_2\gamma^{WL}_{i\longrightarrow j}. \tag{7}$$

Among them, α and β are the weighting coefficients, which are, respectively, expressed as the flow of the straight and turning traffic in each phase:

$$\alpha_1\colon \beta_1\colon \alpha_2\colon \beta_2 = \max\left(Q^T_N, Q^T_S\right)\colon \max\left(Q^L_N, Q^L_S\right)\colon \max\left(Q^T_W, Q^T_E\right)\colon \max\left(Q^L_W, Q^L_E\right). \tag{8}$$

2.2. Definition of Green Wave Bandwidth Coordination Rate. Green wave control is one of the commonly used signal coordination control methods, and its objective function is usually the bandwidth of green wave. However, when the object of coordination is complex, the bandwidth cannot reflect the overall coordination situation well, nor can it reflect the mapping relationship between adjacent intersections. Therefore, this section introduces the green wave bandwidth coordination rate.

Define the green wave bandwidth coordination rate as follows: the ratio of the effective green wave bandwidth between adjacent intersections to the total green time of the downstream intersection in that direction, which can be expressed as

$$\gamma_{ij} = \frac{b_{ij}}{G_j}, \tag{9}$$

where γ_{ij} is the green wave bandwidth coordination rate, b_{ij} is the effective green wave bandwidth between adjacent intersections, and G_j is the total green time of the downstream intersection in that direction.

3. Method and Model

The technical roadmap for the research of the multiroute signal coordination control method considering the green wave bandwidth coordination rate is shown in Figure 3.

3.1. Single Route Control Optimization Model considering Coordination Rate of Green Wave Bandwidth. Considering the research on the signal coordinated control of the road to the route, there is turning behavior in the process of traffic flow, so the green wave bandwidth coordination rate of straight and turning movements is generated, and its upward and downward directions need to be studied separately.

According to the definition, the coordination rate of different green wave bandwidths of adjacent intersections is obtained as follows:

Upstream direct green wave bandwidth coordination rate:

$$\gamma^{ij}_T = \frac{b}{G_j}. \tag{10}$$

Downlink direct green wave bandwidth coordination rate:

$$\overline{\gamma^{ij}_T} = \frac{\overline{b}}{G_i}. \tag{11}$$

Uplink left-turn green wave bandwidth coordination rate:

$$\gamma^{ij}_L = \frac{y_j}{G_j}. \tag{12}$$

Downlink left-turn green wave bandwidth coordination rate:

$$\overline{\gamma^{ij}_L} = \frac{y_i}{G_i}. \tag{13}$$

Among them, b is the straight green bandwidth of the route, and y is the turning green bandwidth at the turning intersection.

The objective function of the route control optimization model based on the green wave bandwidth coordination rate is that the total green wave bandwidth coordination rate in the route is optimal; that is, (2) to (5) are superimposed according to the coordination rate of each connected section of the intersection. The objective function can be expressed as

$$\max \gamma = \sum \alpha\gamma^{ij}_T + \overline{\alpha}\overline{\gamma^{ij}_T} + \beta\gamma^{ij}_L + \overline{\beta}\overline{\gamma^{ij}_L}. \tag{14}$$

Among them, $\alpha, \overline{\alpha}, \beta$, and $\overline{\beta}$ are weighting coefficients, which mean the green wave bandwidth demand ratio for upward straight travel, downward direct travel, upward steering, and downward steering, respectively.

3.2. Basic Multiroute Signal Coordination Control Model. In OD travel, there are often multiple routes for commuters to choose from, and there are situations in which vehicles merge into or out of the arterial road. This results in a situation where multiple routes have overlapping sections. For these situations, only one arterial road is created. The green wave belt is obviously not enough, and it is necessary to create a separate turning green wave belt for the intersection where there is turning behavior. Among them, the route is composed of road segments and nodes.

In this paper, based on the traditional MAXBAND arterial road green wave coordinated control model, the main road traffic turning is considered, and the intersections with

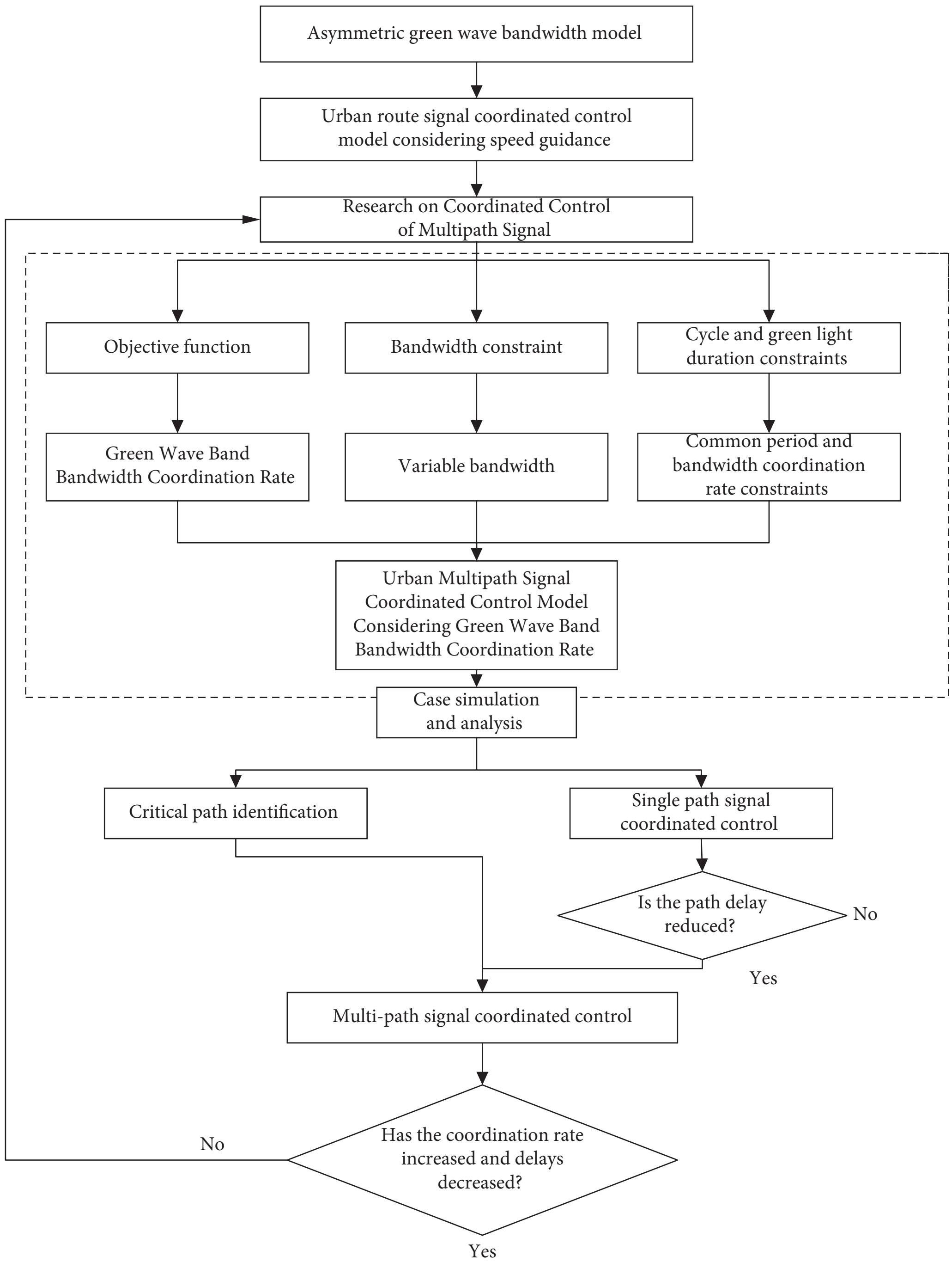

Figure 3: Technology roadmap.

turning traffic flow are separately studied to establish a multiroute signal coordinated control model.

Figure 4 is a time-space diagram of the basic multiroute signal coordination control model OD-BAND, which contains three consecutive intersections involving two-way arterial green waves and three turning routes [21, 22].

The meanings of the parameters in the figure are as follows:

N_i: intersection number.

$b(\bar{b})$: upward (downward) direction, green wave bandwidth between adjacent intersections (s).

$r_i(\overline{r_i})$: at the intersection, the red light time (s) when you leave (enter) the intersection direction.

$w_i(\overline{w_i})$: conflict variables, defined as the start (end) time of the red light and the length of the green wave zone boundary time (s).

$\tau_i(\overline{\tau_i})$: dissipation time of vehicles queuing at downstream intersections (s).

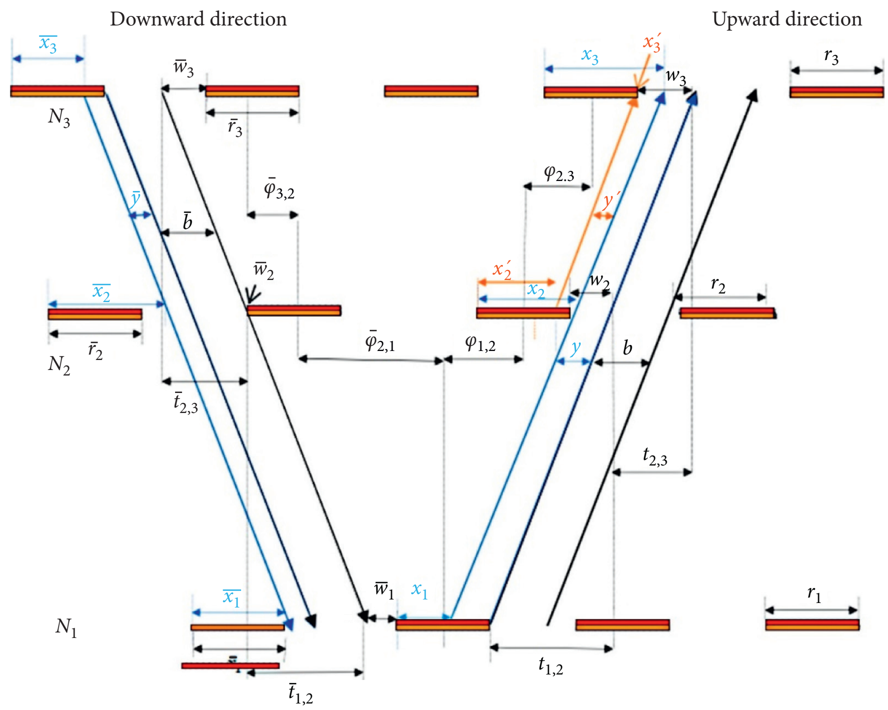

Figure 4: Time-space diagram of coordinated control model for multiroute.

$\Delta_i\,(\overline{\Delta_i})$: red light offset, the difference between time of approaching and departing intersection at the midpoint of the red light (s).

$t_i\,(\overline{t_i})$: travel time in the upward (downward) direction from the current intersection to the downstream intersection (s).

$\phi_i\,(\overline{\phi_i})$: phase difference, defined as the difference at the midpoint of the same phase red light at adjacent intersections (s).

$y, y', \overline{y}$: up and down (downward) direction, adjacent intersections turning to the green wave bandwidth (s).

$x_i\,(x_i')$: the steering bandwidth conflict variable which is the start (end) time of the red light and the length of the boundary time of the steering green wave band (s).

The objective function is

$$\text{Max}B = \alpha b + \overline{\alpha}\overline{b} + by + \overline{b}\overline{y} + b'y'. \quad (15)$$

$\alpha\,(\overline{\alpha})$: uplink (downlink) section saturation constraint.

$\beta\,(\overline{\beta})$: saturation constraint of turning section in the upward (downward) direction.

3.3. Improved Multiroute Signal Coordination Control Model. Since the basic OD-BAND has low applicability and the given model is only for three consecutive intersections, we can make some improvement in it. By including the concept of green wave bandwidth coordination rate mentioned in Section 1, improvements are made from three aspects: variable bandwidth, bandwidth coordination rate constraints, and objective functionalization to expand the applicability and use value of the model.

3.3.1. Variable Bandwidth. The green wave bandwidth coordinated control model is based on the MAXBAND model. Although the green wave bandwidth can be provided in two directions for the arterial, the width of the green wave bandwidth is fixed. However, in actual situations, the timing of each intersection is different, and the green light time is also different. The fixed bandwidth is often the intersection with the highest green light time utilization. The maximum green wave bandwidth is taken as the bandwidth of the entire arterial, which may cause inflexible timing of green lights at other intersections.

In the multiroute signal coordinated control model, the green wave bandwidth can also be changed to increase the control of each intersection.

Define $b_i\,(\overline{b_i})$ as the straight green wave bandwidth in the upstream and downstream directions; $i = N - 1$ is the road section number; the corresponding road section saturation constraint variables are $\alpha_i\,(\overline{\alpha}_i)$ and $\beta_i\,(\overline{\beta}_i)$.

3.3.2. Phase Constraint of Green Wave Bandwidth Coordination Rate. For a general four-phase intersection, the one-way green time is not more than half of the total cycle length [23], which means $G_T^i \le C/2$, so we can define the cycle frequency as $z = 1/C$. According to the formula of the green wave bandwidth coordination rate, the following constraints can be obtained:

$$\begin{aligned} 2zb_i &\le \gamma_T^i \le 1, \\ 2z\overline{b_i} &\le \overline{\gamma_T^i} \le 1, \\ 2zy_i &\le \gamma_L^i \le 1, \\ 2z\overline{y_i} &\le \overline{\gamma_L^i} \le 1. \end{aligned} \quad (16)$$

3.3.3. Objective Function. Take the optimal total green wave bandwidth coordination rate in the multiple routes as the objective function of the model, as shown in the following formula:

$$\max \gamma = \sum_{i=1}^{n-1}\left[\left(a_i \cdot \frac{b_i}{G_T^i}\right) + \left(\overline{a_i} \cdot \frac{\overline{b_i}}{\overline{G_T^i}}\right)\right] + \sum_{j=1}^{p}\left[\sum_{i=1}^{N_D-N_O} \beta_i \frac{y_i}{G_T^i} + \sum_{i=1}^{N_O-N_D} \overline{\beta_i}\frac{\overline{y_i}}{\overline{G_T^i}}\right]. \tag{17}$$

Among them, α, $\overline{\alpha}$, β, and $\overline{\beta}$ are weighting coefficients, which mean the green wave bandwidth demand ratios for upward straight travel, downward direct travel, upward turning, and downward turning, respectively. n is the number of intersections. N_O and N_D are the starting and ending points of the route. $b(\overline{b})$ represents the upstream (downstream) direction, the width of the green band between adjacent intersections. j represents the total number of routes.

Subject to

$$\frac{1}{C_1} \le z \le \frac{1}{C_2},$$

$$(1-k_i)\overline{b}_i \ge k_i(1-k_i)b_i,$$

$$\begin{cases} w_i + b_i \le 1 - r_i \\ \overline{w}_i + \overline{b}_i \le 1 - \overline{r_i} \end{cases},$$

$$(w_i + \overline{w}_i) - (w_{i+1} + \overline{w}_{i+1}) + (t_i + \overline{t}_i) = \frac{1}{2}(r_{i+1} + \overline{r_{i+1}}) - \frac{1}{2}(r_i + \overline{r}_i) + m_i, \quad i = 1, 2, \ldots, n.$$

$$\begin{cases} \left(\dfrac{d_i}{f_i}\right) z \le t_i \le \left(\dfrac{d_i}{e_i}\right) z \\ \left(\dfrac{d_i}{\overline{f_i}}\right) z \le \overline{t}_i \le \left(\dfrac{d_t}{\overline{e_i}}\right) z \end{cases}, \quad i = 1, 2, \ldots, n.$$

$$\begin{cases} \left(\dfrac{d_i}{h_i}\right) z \le \left(\dfrac{d_i}{d_{i+1}}\right) t_{i+1} - t_i \le \left(\dfrac{d_i}{g_i}\right) z \\ \left(\dfrac{\overline{d}_i}{\overline{h}_i}\right) z \le \left(\dfrac{\overline{d}_i}{\overline{d}_{i+1}}\right) \overline{t}_{i+1} - \overline{t}_i \le \left(\dfrac{\overline{d}_i}{\overline{g}_i}\right) z \end{cases}, \quad i = 1, 2, \ldots, n.$$

$$2zb_i \le \gamma_T^i \le 1$$

$$2z\overline{b_i} \le \overline{\gamma_T^i} \le 1 \quad i = 1, 2, \ldots, n-1$$

$$2zy_i \le \gamma_L^i \le 1$$

$$2z\overline{y_i} \le \overline{\gamma_L^i} \le 1 \quad i = N_{O,\ldots,} N_D - 1$$

$$\left(1 - k_i^j\right) \cdot y_i^j \ge \left(1 - k_i^j\right) \cdot k_i^j \cdot b_i$$

$$\left(1 - \overline{k_i^j}\right) \cdot \overline{y_i^j} \ge \left(1 - \overline{k_i^j}\right) \cdot \overline{k_i^j} \cdot \overline{b_i} \quad i = N_{O,\ldots,} N_D - 1$$

$$x_i^j - x_{i+1}^j = w_i - w_{i+1} + r_i - r_{i+1}$$

$$\overline{x_i^j} - \overline{x_{i+1}^j} = \overline{w}_i - \overline{w}_{i+1} + \overline{r_i} - \overline{r_{i+1}} \quad i = 1, 2, \ldots, n-1$$

$$
\begin{aligned}
& y_i^j + x_i^j \le r_i \\
& \overline{y_i^j} + \overline{x_i^j} \le \overline{r_i} \quad i = N_O \\
& x_i^j \ge r_i \quad i = N_O + 1, \ldots, N_D \\
& \overline{x_i^j} \ge \overline{r_i} \quad i = N_D - 1, \ldots, N_O \\
& y_i^j + b_i \le 1 - r_i \\
& \overline{y_i^j} + \overline{b}_i \le 1 - \overline{r_i} \\
& i = N_{O,\ldots,} N_D - 1,
\end{aligned}
\tag{18}
$$

where j is the number of paths; m is an integer; C_1 is the minimum period (s); C_2 is the maximum period (s); k_i is the upstream and downstream bandwidth demand ratio; $b_i\,(\overline{b_i})$ is, in the upward (downward) direction, the width of the green wave band between adjacent intersections; $r_i\,(\overline{r_i})$ is, at an intersection, the length of the red light in the direction of exiting (entering) the intersection; $t_i\,(\overline{t_i})$ is the travel time in the upward (downward) direction from the current intersection to the downstream intersection; $d_i\,(\overline{d_i})$ is the distance between adjacent intersections in the upward (downward) direction (m); $f_i\,(\overline{f_i})$ is the upper limit of the speed in the up (down) direction (km/h); $e_i\,(\overline{e_i})$ is the lower limit of speed in the up (down) direction (km/h); $h_i\,(\overline{h_i})$ is the upper limit of speed fluctuation in the up (down) direction (km/h); $g_i\,(\overline{g_i})$ is the lower limit of the speed fluctuation in the up (down) direction (km/h); and $w_i\,(\overline{w_i})$ is the result of model solution, and its value should usually be greater than half of the green wave bandwidth of the road section. This is an important basis for judging whether the coordination is reasonable.

4. Case Study Analysis

4.1. Simulation Environment. The case selected a road network in the Industrial Park of Suzhou City, Jiangsu Province, China, seen in Figure 5. The east-west arterial road is Zhongyuan Road, and the north and south Wansheng Street, Jinliang Road, Zhongnan Street, etc. form a multi-route road network with vehicles flowing into and out of the arterial road. For investigation during the peak period of traffic flow and signal timing, we used LINGO software programming to solve parameters such as phase difference, green wave bandwidth coordination rate, and conflict variables. In addition, we used Synchro software for road network construction, simulation operation, analysis, and comparison with Synchro's phase optimization plan. The feasibility and advantages of the model were verified.

The intersections are numbered sequentially from left to right, and the involved routes and intersections are shown in Table 1.

4.2. Data Collection. In this paper, the research object selected 11 intersections, 10 road sections, and 5 routes. In order to obtain simulation data, we will start the morning peak at 7:00–9:00 on December 19, 2019, and the evening peak at 17:00 on December 20. At 19:00, the traffic data, entrance cross section, and signal timing of 11 intersections were investigated, the average value of the traffic was taken as the average peak hour traffic, and the subsequent simulation input was carried out. The flow data and signal timing of the entrance lanes of each intersection are shown in Tables 2 and 3.

The intersections S_1–S_{11} correspond to the intersections, respectively, of Zhongyuan Road–Xinghu Street, Zhongyuan Road–Wansheng Street, Wangdun Road–Wansheng Street, Zhongyuan Road–Nanshi Street, Zhongyuan Road–Jinliang Street, Zhonghui Road–Jinliang Street, Zhonghui Road–Xinghu Street, Zhongyuan Road–Liuli Street, Zhongyuan Road–Zhongnan Street, Zhaojia Alley–Zhongnan Street, and Zhongyuan Road–Jinxi Street.

4.3. Model Solution. According to the programming solution of the model by LINGO software, the straight green wave bandwidth coordination rate and the turning green wave bandwidth coordination rate of each intersection are shown in Tables 4 and 5.

4.4. Results Discussion. Through simulation analysis, the delays of each intersection after model optimization and Synchro optimization are obtained, such as the delay and phase difference of the intersection, seen in Table 6.

After calculation, the average delay of the intersection obtained by Synchro's optimization model is 29.2 s, and the average delay of the intersection of the model studied in this paper is 28.03 s. From the table, it can be seen that intersection I and intersection XI are the main roads within the scope of the study, and they bear greater traffic pressure; intersections II, IV, V, and IX are important nodes involved in the turning route, and their delays are also relatively high.

Through simulation analysis, the delays of each intersection after model optimization and Synchro optimization are obtained. The comparison is shown in Figure 6.

It can be seen from the figure that among the I–XI intersections in the study range, except for intersections V, VIII, and X, the intersection delays after the optimization of the model scheme in this paper are all lower than those after Synchro optimization. The intersection delay obtained by the overall model is 4.3% lower than the average intersection delay obtained by Synchro optimization.

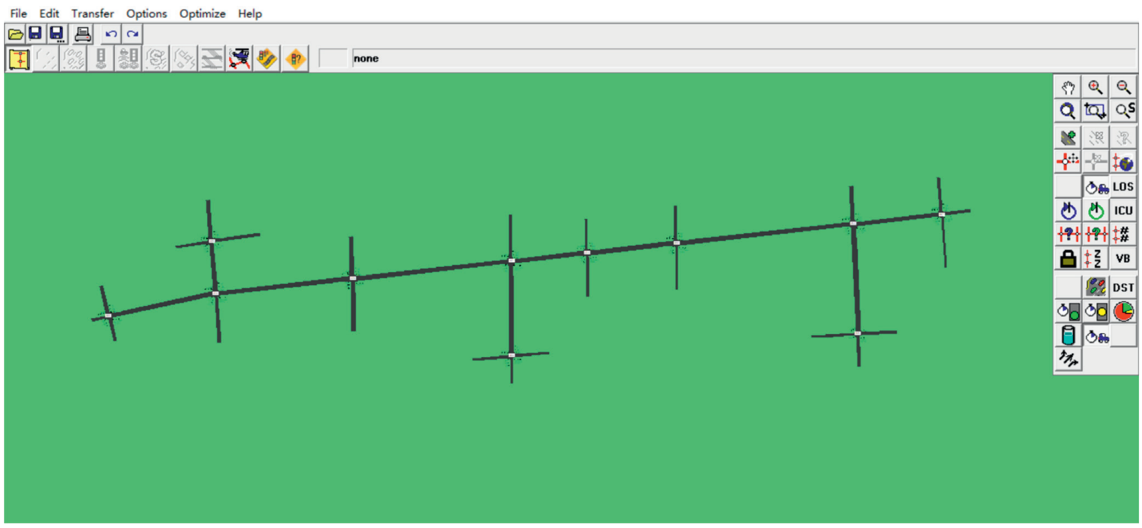

Figure 5: Case road network model in Synchro.

Table 1: Origins, destinations, and routes in the case road network.

Travel point	Arrival point	Route
1	11	1-2-4-5-7-8-9-11
3	6	3-2-4-5-6
3	10	3-2-4-5-7-8-9-10
10	1	10-9-8-7-5-4-2-1
11	1	11-9-8-7-5-4-2-1

Table 2: Traffic volume at case intersections (pcu/h).

Intersection	South import			North import			East import			West import		
	Left	Straight	Right	Left	Straight	Right	Left	Straight	Right	Left	Straight	Right
S_1	285	320	169	195	396	190	138	149	162	119	227	182
S_2	266	755	276	112	178	266	263	217	182	134	194	237
S_3	135	337	262	135	330	151	50	190	245	123	260	204
S_4	128	333	131	368	647	153	100	144	164	123	260	204
S_5	304	253	277	225	297	244	181	344	236	89	203	344
S_6	162	298	360	129	185	306	129	169	250	237	464	393
S_7	134	276	244	175	166	272	111	291	227	210	423	333
S_8	234	249	117	149	169	236	315	241	151	176	172	170
S_9	156	418	229	223	389	105	299	243	189	246	369	266
S_{10}	107	397	111	127	334	121	102	168	79	98	172	56
S_{11}	187	407	198	232	379	201	287	346	196	257	356	203

Table 3: Current signal timing plan at case intersections.

Intersection	First phase (s)	Second phase (s)	Third phase (s)	Fourth phase (s)	Period (s)
S_1	East-west straight, right/21	Turn left from east to west/12	North-south straight, right/22	Turn left from north to south/20	75
S_2	East-west straight, right/20	Turn left from east to west/17	North-south straight, right/21	Turn left from north to south/17	75
S_3	East-west straight, right/21	Turn left from east to west/13	North-south straight, right/23	Turn left from north to south/13	70
S_4	East-west straight, right/20	Turn left from east to west/11	North-south straight, right/19	Turn left from north to south/20	70
S_5	East-west straight, right/20	Turn left from east to west/12	North-south straight, right/20	Turn left from north to south/18	70

Table 3: Continued.

Intersection	First phase (s)	Second phase (s)	Third phase (s)	Fourth phase (s)	Period (s)
S_6	East-west straight, right/25	Turn left from east to west/16	North-south straight, right/20	Turn left from north to south/14	75
S_7	East-west straight, right/22	Turn left from east to west/14	North-south straight, right/22	Turn left from north to south/12	70
S_8	East-west straight, right/22	Turn left from east to west/21	North-south straight, right/20	Turn left from north to south/17	80
S_9	East-west straight, right/24	Turn left from east to west/20	North-south straight, right/20	Turn left from north to south/16	80
S_{10}	East-west straight, right/27	North-south straight, right/24	Turn left from north to south/19	—	70
S_{11}	East-west straight, right/21	Turn left from east to west/19	North-south straight, right/24	Turn left from north to south/16	80

Table 4: Coordination rate of green wave bandwidth and offsets in the arterial.

Intersection	Uplink green wave bandwidth coordination rate	Downlink green wave bandwidth coordination rate	Phase difference (s)
I	—	0.44	27
II	0.58	0.48	8
III	—	—	72
IV	0.42	0.48	3
V	0.41	0.42	2
VI	—	—	40
VII	0.52	0.39	42
VIII	0.43	0.57	38
IX	0.49	0.39	45
X	—	—	8
XI	0.52	—	15

Table 5: Coordination rate of green wave bandwidth and offsets for turning movement.

Intersection	Shift to green wave bandwidth coordination rate	Intersection	Shift to green wave bandwidth coordination rate
I	0.49	7	0.42
II	0.49	8	0.44
IV	0.45	9	0.37
V	0.43	10	0.42
VI	0.49	—	—

Table 6: Intersection delay and phase difference.

Intersection	Synchro optimization model		This article research model	
	Phase difference (s)	Delay (s)	Phase difference (s)	Delay (s)
I	71	31.7	27	31.0
II	8	26.7	8	25.5
III	72	19.6	72	18.9
IV	0	33.3	3	25.8
V	5	26.4	2	27.6
VI	37	28.6	40	28.3
VII	56	25.0	42	23.7
VIII	38	30.5	38	32.1
IX	43	33.5	45	31.2
X	2	19.2	8	18.5
XI	10	47.1	15	45.7
Overall benefit	—	29.24	—	28.03

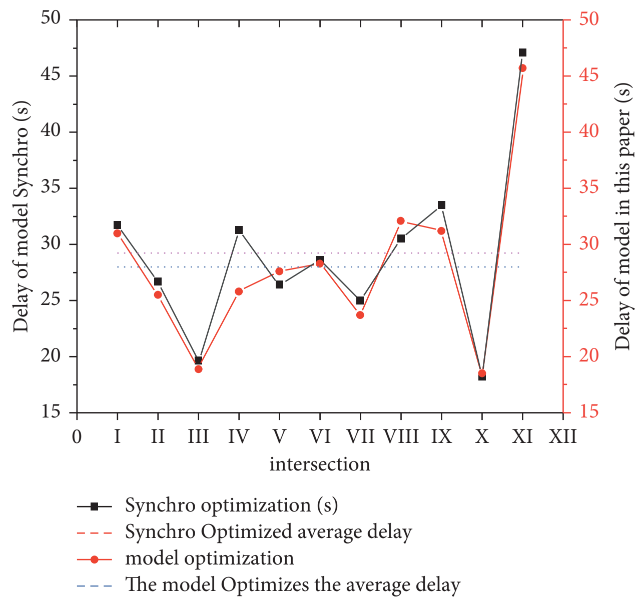

Figure 6: Comparison of intersection delay between the model in the paper and the model in Synchro.

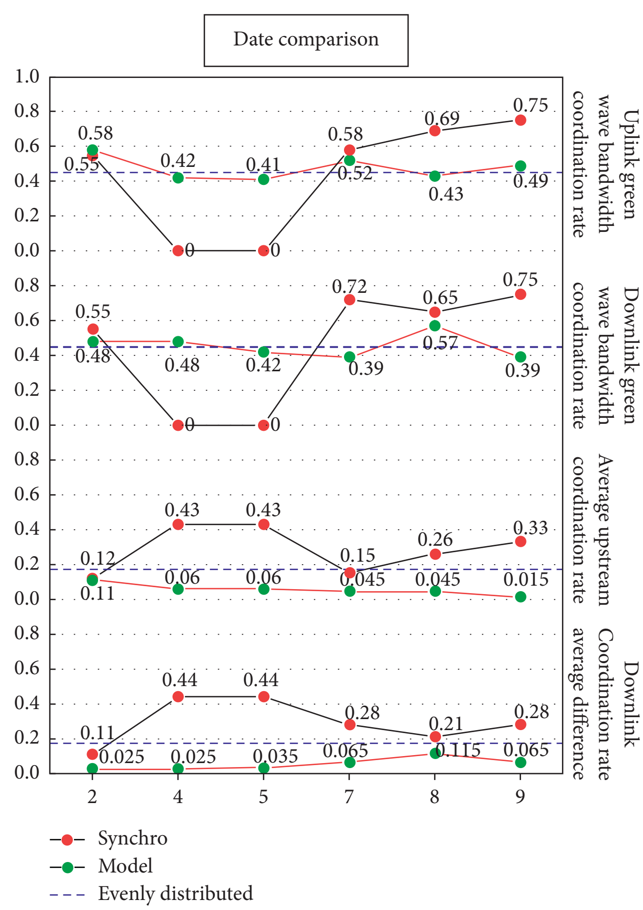

Figure 7: Comparison of coordination rate of green wave bandwidth between the model in the paper and the model in Synchro.

Since Synchro lacks the optimization of route turning bandwidth and the concept of coordination rate, in order to evaluate the overall optimization results, the intersection in the arterial is selected as the reference comparison basis, and the green wave bandwidth in the arterial after optimization based on the Synchro model crosses the downstream. The green light duration of this phase at the intersection is obtained, and the green wave bandwidth coordination rate of the

Table 7: Comparison of evaluation indexes.

Program	Total route delay (hr)	Total number of stops (times)	Average speed (km/h)
Model in Synchro	37.7	4192	23.77
Model in this paper	36.5	4166	25.02

corresponding intersection is obtained, which is analyzed and compared with the green wave bandwidth coordination rate obtained by the LINGO software programming in the model in this paper. The result is shown in Figure 7.

From top to bottom, the figure shows the uplink green wave bandwidth coordination rate, downlink green wave bandwidth coordination rate, average uplink green wave bandwidth coordination rate, and average downlink green wave bandwidth coordination rate of the Synchro scheme and the model scheme studied in this article. Due to Synchro's lack of turning optimization of the green wave, the main road intersections are compared and studied. The green wave bandwidth coordination rate obtained by the model in this paper is more stable and continuous, and the mean difference distribution curve is also more stable, with a fluctuation range of 0.025 to 0.115. The results obtained by Synchro fluctuate greatly, deviating from the mean line, and the maximum difference between the upper and lower limits of the fluctuation is 0.33.

Therefore, in the actual road network, where there are many intersections and multiple routes, the disadvantage of classical Synchro model is only to optimize the overall route, with no relationships between intersections. Moreover, in Synchro, there is not much difference between the upstream and downstream bandwidth. At the same time, the demand ratio of traffic in real world is not considered, which results in more delay.

The model in this paper, from the perspective of the overall continuity of the green wave bandwidth, has stronger applicability and can reduce or avoid the workload and research errors caused by the division of coordination subregions. In general, the coordination effect is also better.

Through the simulation operation, the evaluation indexes of the total route delay, the total number of stops, and the average vehicle speed are obtained, as shown in Table 7.

According to the simulation results, the total route delay in this paper is 36.5 hr. Compared with Synchro's optimization solution, the delay is reduced by 3.3% and 15% compared with the current situation. In terms of total parking times, compared with Synchro's optimization solution, it is reduced by approximately 30 times; in terms of average vehicle speed, compared to the Synchro optimization solution, it has increased by 1.3 km/h.

5. Conclusion

According to the characteristics of phase mapping, the concept of green wave bandwidth coordination rate was first proposed in this paper. Moreover, based on the classic arterial coordinated control model MAXBAND, we proposed an improved multiroute signal coordinated control model, which is suitable for inbound, outbound, and turning movement of commuting traffic. In the model, objective function, variable bandwidth, and coordination rate constraint of green wave bandwidth were discussed in detail, and finally we solved the model as a mixed integer linear programming problem.

The model proposed in this paper takes the green coordination rate of wave bandwidth as the objective function. When the research object becomes complex such as multiroute or regional road network, it can more intuitively reflect the overall coordination situation and can also reflect the coordination of adjacent intersections according to its mapping characteristics.

From the case study, we can conclude that the green wave bandwidth in arterial gotten from the model in this paper is more continuous and stable, and each turning route also has an independent turning bandwidth, which can be better applied in a multiroute environment.

Data Availability

All the data used to support the findings of this study are included in Tables 2 and 3 in this article.

Conflicts of Interest

The authors declare that they have no conflicts of interest.

Acknowledgments

The authors acknowledge with thanks the financial support of this research by the Natural Science Foundation of Shanghai: 20ZR1439300.

References

[1] J. D. C. Little, M. D. Kelson, and N. M. Gartner, *MAXBAND: A Program for Setting Signals on Arteries and Triangular Networks*, Transportation Research Board, Washington, D.C., USA, 1981.

[2] R. E. Allsop, "Choice of offsets in linking traffic signals," *Traffic Engineering and Control*, vol. 10, no. 2, pp. 73–75, 1968.

[3] M. Dotoli, M. P. Fanti, and C. Meloni, "A signal timing plan formulation for urban traffic control," *Control Engineering Practice*, vol. 14, no. 11, pp. 1297–1311, 2006.

[4] N. H. Gartner, S. F. Assmann, F. Lasaga, and D. L. Hou, "MULTIBAND—a variable-bandwidth arterial progression scheme," *Transportation Research Record Journal of the Transportation Research Board*, vol. 287, pp. 212–222, 1990.

[5] C. Stamatiadis and N. Gartner, "MULTIBAND-96: a program for variable-bandwidth progression optimization of multiarterial traffic networks," *Transportation Research Record: Journal of the Transportation Research Board*, vol. 15, no. 54, pp. 9–17, 1996.

[6] Z. Chao, Y. Xie, N. H. Gartner, C. Stamatiadis, and T. Arsava, "AM-Band: an asymmetrical multi-band model for arterial traffic signal coordination," *Transportation Research Part C*, vol. 58, pp. 515–531, 2015.

[7] S. D. Lu and L. Cheng, "Optimization of bidirectional green wave coordinated control graphical method under asymmetric phase sequence mode," *Journal of Highway and Transportation Research and Development*, vol. 32, no. 1, pp. 128–132, 2015.

[8] A. Tugba, X. Yuanchang, and G. Nathan, "OD-NETBAND: an approach for origin–destination based network progression band optimization," *Transportation Research Record: Journal of the Transportation Research Board*, vol. 2672, no. 18, pp. 58–70, 2018.

[9] R. T. V. Katwijk, B. D. Schutter, and J. Hellendoorn, "Multi-agent control of traffic networks: algorithm and case study," in *Proceeding of the International IEEE Conference on Intelligent Transportation Systems*, pp. 316–321, IEEE, St. Louis, MO, USA, 2009.

[10] Y. S. An, *Signal Optimization of Urban Main Road and Surrounding Area Based on Coordinated Control of Several Critical paths[D]*, SHANDONG UNIVERSITY, Jinan, China, 2018.

[11] Z. Liang, Y. Xiao, and Y.-P. Flötteröd, "An overlapping phase approach to optimize bus signal priority control under two-way signal coordination on urban arterials," *European Transport Research Review*, vol. 2021, pp. 1–13, 2021.

[12] Y. Y. Zhang, J. L. Li, and Z. Yibing, "Study on green wave coordination control method based on ripple changes," *Journal of Transportation Engineering and Information*, vol. 17, no. 3, pp. 52–61, 2019.

[13] S. P. Zhou, H. R. Li, Z. Qi, G. Meng, and R. Bin, "Traffic signal coordination control optimization considering vehicle emissions on urban arterial road," *Journal of Computational Methods in Science and Engineering*, vol. 21, no. 1, pp. 233–239, 2021.

[14] L. Wen, B. T. Dong, P. Li, and Y. An, "Signal coordination control based on comprehensive correlation degree," *IOP Conference Series: Earth and Environmental Science*, vol. 638, no. 1, pp. 1–8, 2021.

[15] H. T. Xu, Z. Z. Zhuo, J. Chen, and X. Fang, "Traffic signal coordination control along oversaturated two-way arterials," *PeerJ. Computer science*, vol. 6, pp. 1–22, 2020.

[16] G. J. Shen and Y. Y. Yang, "A dynamic signal coordination control method for urban arterial roads and its application," *Frontiers of Information Technology & Electronic Engineering*, vol. 17, no. 9, pp. 907–918, 2016.

[17] L. Lu, J. G. Gu, Q. Fu, and Y. Li, "Study on cooperative control method among large flow and long-distance intersections," *Applied Mechanics and Materials*, vol. 3843, pp. 2006–2011, 2015.

[18] H. Lan and X. Wu, "Research on Key Technology of signal control subarea partition based on correlation degree analysis," *Mathematical Problems in Engineering*, vol. 2020, pp. 1–12, 2020.

[19] A. I. Croce, G. Musolino, C. Rindone, and A. Vitetta, "Route and path choices of freight vehicles: a case study with floating car data," *Sustainability*, vol. 12, pp. 1–15, 2020.

[20] H. T. Hu, *Optimal Control of Regional Traffic Signals Based on Phase Difference Coordination Mechanism [D]*, Nanjing University of Posts and Telecommunications, Nanjing, 2018.

[21] T. Arsava, Y. Xie, N. H. Gartner, and J. L., "Arterial Traffic Signal Coordination Utilizing Vehicular Traffic Origin-Destination information," in *Proceeding of the International IEEE Conference on Intelligent Transportation Systems*, pp. 8–11, IEEE, Qingdao, China, 2014.

[22] E. Jenelius and L. G Mattsson, "Developing a Methodology for Road Network Vulnerability analysis," in *Proceeding of the Nectar Cluster 1 Meeting*, pp. 1–9, Molde, Norway, 2006.

[23] K. P. Li, *Traffic Signal Control Guidelines-Current German Specifications (RiLSA)*, China Architecture & Building Press, Beijing, China, 2006.